



# Dynamic train-track interactions over track stiffness discontinuities in railway track transitions mitigated by resilient materials

Surapan Noppharat<sup>1</sup> · Anand Raj<sup>1</sup> · Chayut Ngamkhanong<sup>1,2</sup> · Ting Li<sup>3</sup> · Ruilin You<sup>4</sup> · Sakdirat Kaewunruen<sup>5</sup>

Received: 8 April 2024 / Accepted: 2 July 2024 / Published online: 29 July 2024  
© Springer Nature Switzerland AG 2024

## Abstract

Railway track transitions, where abrupt changes between different track sections lead to differential settlement and increased maintenance costs, pose a significant challenge. This often results in considerable track damage and elevated maintenance expenses. In Thailand, the early stages of the high-speed rail project integrate a slab track system from China with conventional ballasted tracks at multiple junctions, underscoring the importance of effectively managing these transition zones. Despite the potential benefits of Under Sleeper Pads (USPs) in ballasted tracks and Under Slab Mats (USMs) in slab tracks for reducing track vibration, impact load, and differential settlement, their usage is not widespread. This paper presents a 3D train-track-soil finite element model that incorporates both USPs and USMs, considering strain-rate effects, to analyze railway track transitions. The model evaluates various pad types across different track locations and train speeds. The results show that USPs can significantly reduce ballast degradation, while USMs help maintain overall track stiffness. The results also show that the combination of USPs and USMs effectively manages track stiffness gradients, achieving a normalized gradient between 0.04 and 0.20, compared to 1.00 in the baseline case. Although the combined use of USPs and USMs offers a promising solution for managing track transitions, careful selection are crucial to avoid potential issues. This research provides a comprehensive framework for understanding and improving the performance of railway track transition zones using resilient materials. It suggests further studies to evaluate the broader applicability of these methods in minimizing track disturbances across various environmental conditions.

**Keywords** Track transition · Dynamic analysis · Train-track-soil interactions · Under sleeper pads (USPs) · Under slab mats (USMs)

---

✉ Chayut Ngamkhanong  
Chayut.ng@chula.ac.th

Surapan Noppharat  
S.Noppharat@outlook.com

Anand Raj  
anandrajce@gmail.com

Ting Li  
liting9225@126.com

Ruilin You  
youruilin0731@126.com

Sakdirat Kaewunruen  
s.kaewunruen@bham.ac.uk

<sup>1</sup> Department of Civil Engineering, Faculty of Engineering, Chulalongkorn University, Bangkok, Thailand

<sup>2</sup> Advanced Railway Infrastructure, Innovation and Systems Engineering (ARIISE) Research Unit, Chulalongkorn University, Bangkok, Thailand

<sup>3</sup> Key Laboratory of Roads and Railway Engineering Safety Control, Ministry of Education, Shijiazhuang Tiedao University, Shijiazhuang 050043, China

<sup>4</sup> Railway Engineering Institute, China Academy of Railway Sciences, Beijing 100081, China

<sup>5</sup> School of Civil Engineering, University of Birmingham, Birmingham B15 2TT, UK

## Introduction

Engineering advancements in construction technologies have led to the development of efficient transportation systems, and railway infrastructure is at the forefront of this trend. Rail transportation has several advantages over other modes of transportation, such as high load capacity, punctuality, and convenience [1]. The developments of railway infrastructure are crucial for driving economic growth and social development.

Recently, Thailand has adopted a new construction technology from China, the Chinese Railway Track System (CRTS) type III, for the first phase of high-speed rail line project. However, there are concerns regarding the design and construction of the railway track system, particularly the issue of track transition. The route for the project includes a region where the track section changes from ballasted track to slab track. Changing the track section abruptly can cause a sudden change in the vertical track stiffness of the structures, leading to an increase in dynamic forces, vertical acceleration and thus reduce passenger comfort at particular sections. Additionally, considering the context of Bangkok's soil composition, the characteristics predominantly exhibit clay or soft soil attributes. This makes differential settlement more pronounced, which poses a significant challenge for track transitions on soft soil. Track transitions on soft soil, such as those found in Bangkok, can lead to severe track irregularities and increased maintenance demands. The soft soil's low bearing capacity and high compressibility exacerbate differential settlement, causing uneven track support and alignment issues.

In the past, several solutions, such as pile [2], subgrade modification [3], fastening system [4], Hot-Mixed Asphalt [5], and approach slab [6], have been proposed to solve track transition problems. However, these methods are cost effective and difficult to install after the tracks have been constructed [7]. Numerous studies have employed the Finite Element Method (FEM) in conjunction with field measurements to address issues related to the transition zone, applying diverse methodologies for more effective solutions [8–10]. It should be noted that the selection of solutions can differ based on objectives, expenses, and accessibility.

A comprehensive study exploring three approaches was conducted to minimize rail displacement during the transition from ballasted track to slab track [11]. Notably, their findings highlight that modifying the track stiffness through subgrade adjustments emerges as the most impactful method for enhancing vertical stiffness along the track. Additionally, the incorporation of auxiliary rail offers a promising avenue to fine-tune stress distribution, acceleration patterns, and track displacement. Ngamkhanong et al. (2020) [12] conducted research focusing on the implementation

of baseplate fastening systems to mitigate vibrations in the transition zone. They compared their study's outcomes with those of other research efforts, encompassing both ballasted Track and slab Track systems. The research was categorized based on baseplate stiffness and weight, and it also investigated the arrangement of base plates along the transition to ensure consistent alterations in rail displacement and track stiffness.

Paixão et al. (2018) conducted a study using numerical simulation to enhance vibration control at bridge ends [13]. They focused on track transition junctions between soil layers and bridge structures, implementing USPs to mitigate vibrations. The study aimed to understand USPs impact on railway structure behavior and investigate abnormal stiffness increases before transitions. Rail displacement and sleeper acceleration values were high during these transitions. USPs effectively reduced vibrations, with optimized USPs leading to consistent stiffness. This resulted in improved wheel-rail force and vertical acceleration continuity in soil layers at various track transition sections.

The behavior and impact of resilient materials, including USPs and UBMs, across different moisture conditions have been explored. Various tests were conducted, such as static test, dynamics test, and impact modal test, to ascertain the most appropriate material properties for potential future applications. The research concluded that Medium USPs and Stiff USPs were the recommended types of pads to address these challenges. These pads demonstrated compatibility with the desired properties, with a recommended Bedding Modulus range of 0.15 to 0.35 N/mm<sup>3</sup> [14]. The recommended applications of USPs and UBMs corresponding to bedding modulus are presented in Tables 1 and 2. It is found that these pads are categorized from soft to stiff types. However, previous study suggested that a new category of USP, termed "Very stiff," could be introduced, characterized by a bedding modulus of over 0.35 N/m<sup>3</sup> [15]. This classification proves advantageous, particularly under conditions of extremely high impact load. Notably, the implementation of this category avoids substantial sleeper excitation, simultaneously diminishing ballast stress.

CRTS-type III slab track represent a cutting-edge solution on slab track system developed in China with the layers of Self Compacting Concrete (SCC) and isolation layer instead of Calcium Aluminate (CA) mortar [16, 17]. These materials effectively disperse vibrations across concrete slabs and underlying structures, thereby ensuring prolonged structural integrity throughout the track's operational lifespan [18]. Incorporating this technology involves strategically placing isolation layer's rubber materials between layers of Self-compacting Concrete and concrete base within the CRTS-type III slab track configuration. Through these advancements, railway systems can benefit from improved

**Table 1** Under sleeper pads (USPs) applications and characterizations [14]

USP applications and characterizations	Very Soft	Soft	Medium	Stiff
Static bedding modulus, $C_s$ [N/mm <sup>3</sup> ]	$C_s \leq 0.10$	$0.10 < C_s \leq 0.15$	$0.15 < C_s \leq 0.25$	$0.25 < C_s \leq 0.35$
Improve Track Quality (Reduce Ballast Breakage and Track/Turnout Pressure)			✓	✓
Transition Zones			✓	✓
On Existing Structures with Reduced Ballast Thickness			✓	✓
Reduction of Long-Pitch low Rail Corrugation in Tight Curves			✓	✓
Reduction of Ground-Borne Vibration		✓	✓	

**Table 2** Under ballast mats (UBMs) applications and characterizations [14]

UBM Applications and Characterizations	Very Soft	Soft Medium	Medium Stiff	Stiff
Dynamic Bedding Modulus, $C_d$ [N/mm <sup>3</sup> ]	$0.03 < C_d \leq 0.05$	$0.05 < C_d \leq 0.09$	$0.09 < C_d \leq 0.22$	$0.22 < C_d$
Vibration Reduction and Ground-borne Noise	✓	✓		
Ballast Breakage Protection		✓		
On Existing Structures with Reduced Ballast Thickness				✓
Transition Zones				✓

resilience, reduced maintenance needs, and optimized long-term performance [19]. However, only a few studies have been presented previously regarding the stiffness variation and mechanical properties of isolation layer on CRTS-type III slab track. Previous studies showed that the thickness of an isolation layer is relatively small, and it is not significantly compressed during regular operation. This implies that their elastic properties might not be very pronounced, but they are used for layer separation. Therefore, the rubber Under Ballast Mats (UBMs) was recommended to be used as an isolation layer in slab track so called “Under Slab Mat (USMs)” [20]. By using rubber-based materials, such as UBMs, as an isolation layer, it is likely that the elastic properties of the material can provide better vibration damping and isolation performance compared to the thinner layers mentioned earlier.

Note that open literature on solving transition problems with coupling methods is very limited. Therefore, in this study, we propose a coupling method using several types of nonlinear resilient materials that are made of natural rubber such as Under Sleeper Pads (USPs) and Under Slab Mats (USMs) to address this problem. It is important to note that this paper is the first to integrate USMs considering stiffness variation as isolation layer in slab track CRTS type III panels in the dynamic train track interaction model. However, while the incorporation of resilient materials is intended to improve track stiffness discontinuities, it may have a trade-off effect by potentially softening the track if not properly utilized. The Bangkok Soft Clay, known for its high compressibility and low shear strength, presents a particularly critical challenge in this context. This type of soil can significantly impact the stability and performance of railway track structures, making the careful selection

and precise implementation of materials like Under Sleeper Pads (USPs) and Under Slab Mats (USMs) essential. If these materials are not correctly applied, the anticipated benefits, such as reducing differential settlement and track vibration, could be compromised. Instead of enhancing track stability, improper use could lead to excessive track flexibility, thereby diminishing overall track performance. By incorporating Bangkok Soft Clay into our dynamic train-track interaction model, we aim to simulate real-world conditions more accurately, reflecting the unique challenges posed by this soil type. In this study, a prevalent and effective method involves utilizing Nonlinear Finite Element Analysis (FEA) considering the effects of strain-rate where previous research has not adequately explored. This technique is then benchmarked against field measurements for each unique problem scenario. This approach offers both enhanced simplicity and heightened realism, focusing particularly on the application of resilient materials like Under Sleeper Pads (USPs) and Under Slab Mats (USMs) installed at transition zone.

### Methodology

In this paper, develop 3D Finite Element Method (FEM) models of railway track transition with the consideration of train, track and ground using LS-DYNA, as shown in Fig. 1. The figure illustrates the comprehensive finite element model of the railway track transition zone, encompassing the train, track, and ground layers. This model integrates several critical components to accurately simulate the dynamic interactions in the transition zone. In this study, nonlinear dynamic train-track interaction analyzes are performed under various train speeds. The focus of the

**Fig. 1** Fully coupled of train-track-soil system of track transition model in LS-DYNA

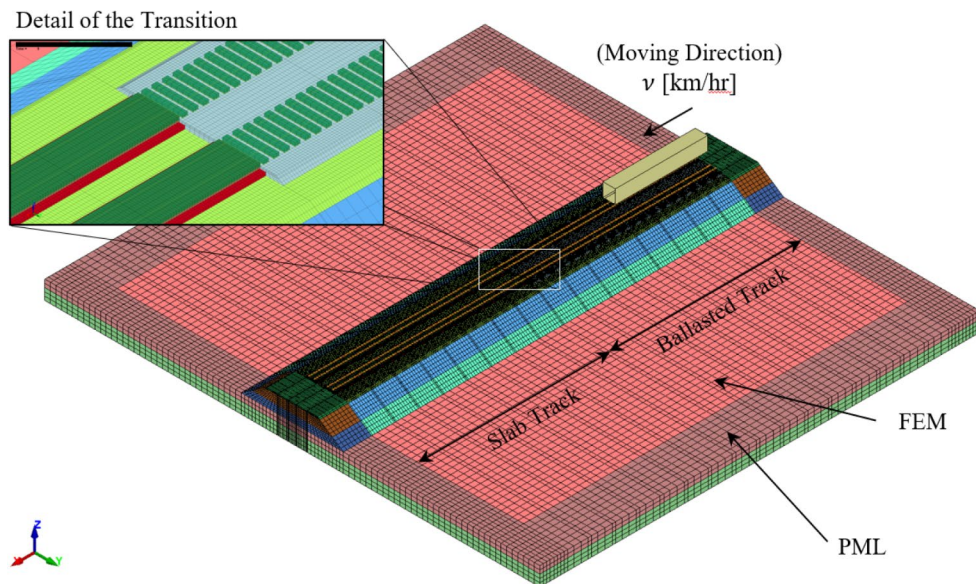


**Table 3** Properties of CR 400BF, Fuxing-Hao EMU train [22]

Properties	Value	Unit
Mass of Car Body	45,200	kg
Mass of Bogie Frame	2,276	kg
Mass of Wheelset	1,627	kg
Inertia of Pitch Motion of the Car Body	$5.47 \times 10^5$	kg.m <sup>2</sup>
Inertia of Pitch Motion of the Bogies	$6.80 \times 10^3$	kg.m <sup>2</sup>
Primary Suspension Stiffness, $K_1$	$1.04 \times 10^6$	N/m
Primary Suspension Damping, $C_1$	$5.00 \times 10^3$	N.s/m
Secondary Suspension Stiffness, $K_2$	$4.00 \times 10^5$	N/m
Secondary Suspension Damping, $C_2$	$6.00 \times 10^3$	N.s/m

analysis is on the track transition zone, where USPs and USMs are installed. This section includes train modelling, track modelling, ground modelling and USPs and USMs. In each section of this study, we present the finite element model with detailed descriptions of the material models, section properties, and material characteristics for various parts of the system. This includes comprehensive modeling of the train, track, ground layers, USPs and USMs used in the transition zones. Initially, the model’s material properties, especially those of the train and soil, are carefully adjusted and validated against existing studies to ensure accuracy and reliability. This validation phase is crucial for establishing a credible baseline that reflects real-world conditions. Following this, the model is specifically adapted to address the challenges posed by soft soil conditions, typical in the Bangkok region. This adaptation involves fine-tuning the soil parameters to accurately simulate the behavior of dynamic train-track interactions over transition zone.

### Train modelling

The train model is developed based on multi-body simulations and consists of three main components: car body, bogies, and wheelsets. The first component is the car body modelled as a rigid body using shell element. The second component models the bogies using shell elements. The third component models the wheelsets are modelled using beam elements. These components are connected through a suspension system composed of a spring and damper or discrete element. This study considers the CR400 BF, Fuxing-Hao EMU train, which has similar rolling stock parameters to those of the highspeed trains adopted for the project in Thailand. The vehicle properties are presented in Table 3.

To analyze the vertical response, Fig. 2 presents the train model, which has 10 Degree of Freedom (DOFs) including the vertical translation and rotation of one rigid car body ( $Z_c, \beta_c$ ), the vertical displacement and rotation of two bogies ( $Z_{bi}, \beta_{bi}; i = 1, 2$ ), and the vertical translation of four wheelsets ( $Z_{bi}; i = 1, 2, 3, 4$ ) [21]. Note that we mainly aim to examine the vertical displacement and rotation of these specific parts to better understand the train’s vertical response so that the transverse translation and rotation are neglected.

### Track modelling

At transition zone, the track section is divided into two: slab track and ballasted track. The overall track section is 100 m long consisting of 50 m ballasted track and 50 m slab track. Steel rails are modelled using beam element and are connected to rail pads and fasteners, which are modelled using spring and discrete spring elements. In order to accurately capture behavior of the system, the effect of irregularities is included in the rail model. It is computed using the Power

**Fig. 2** Degree of freedom (DOFs) of train model

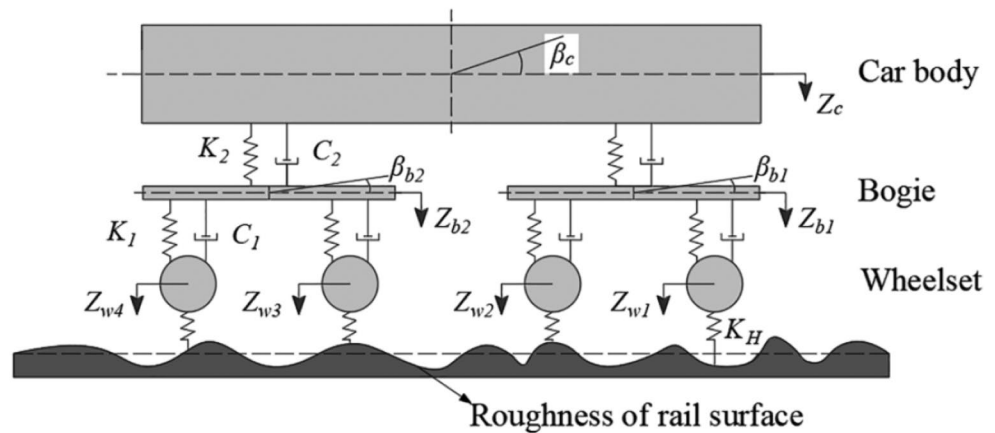


**Fig. 3** Roughness with distance and PSD wavelength [24]

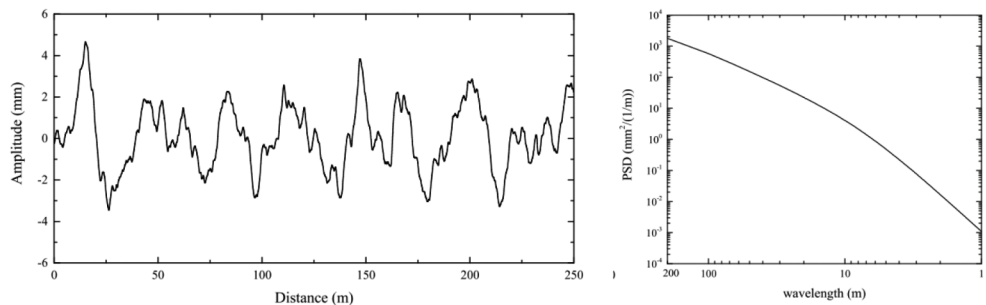
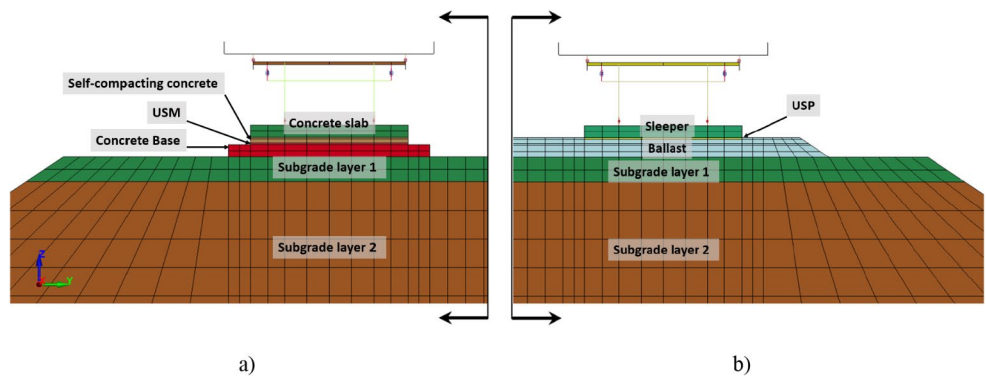


**Fig. 4** Track cross sections (a) Slab track CRTS type III with USMs, (b) Ballasted track with USPs



Spectrum Density (PSD) Function, as shown in Eq. 1. It is noted that the parameters used has been validated using data from Germany’s high-speed rail low disturbance network [23, 24], ensuring that the model accurately represents the behavior of the rail system. Figure 3 presents the track irregularity along the distance.

$$S_v(\Omega) = \frac{A_v \Omega_c^2}{(\Omega^2 + \Omega_r^2)(\Omega^2 + \Omega_c^2)} \tag{1}$$

Where  $A_v$  = Roughness Constant ( $4.032 \times 10^{-7} \text{ m}^2 \cdot \text{rad/m}$ ).  
 $\Omega$  = Spatial Frequency of the Roughness.  
 $\Omega_c$  = Cutoff Frequency (0.8246 rad/m).  
 $\Omega_r$  = Cutoff Frequency (0.0206 rad/m).

Ballasted tracks consist of various components, including rails, sleepers, USPs and ballast. Additionally, slab tracks of CRTS type III feature reinforced concrete slabs, a filling layer of self-compacting concrete, USMs and a supporting layer of plain concrete (concrete base). Both ballasted and slab tracks sit on similar subgrade layers. Note that the beam element is considered for rails and discrete spring element is considered for fastening system while the 3D solid element is considered for other components. Figure 4 presents the cross section of both slab and ballasted tracks where mesh is also presented.

Tables 4 and 5 contain all the material and section properties for the ballasted track and slab track, respectively, that are utilized in the analysis. It is important to note that the dynamic properties with strain-rate dependent are considered using the keyword STRAIN\_RATE\_DEPENDENT\_PLASTICITY,

**Table 4** Material properties of ballasted track

Properties	Value	Unit
Mass Density of the Ballast	1800	kg/m <sup>3</sup>
Poisson's Ratio of the Ballast	0.30	mm/mm
Modulus of Elasticity of the Ballast	1.50 × 10 <sup>8</sup>	N/m <sup>2</sup>
Mass Density of the Sleeper	2400	kg/m <sup>3</sup>
Poisson's Ratio of the Sleeper	0.25	mm/mm
Modulus of Elasticity of the Sleeper **	3.00 × 10 <sup>10</sup>	N/m <sup>2</sup>
Stiffness of the Rails Pads *	5.0 × 10 <sup>7</sup>	N/m
Damping of the Rail Pads	7.5 × 10 <sup>4</sup>	N.s/m
Mass Density of the Rail Pads	1500	kg/m <sup>3</sup>

\*Dynamics stiffness

\*\* Reference static value, Strain rate dependent

**Table 5** Material properties of slab track, CRTS type III (Wang et al., 2017)

Properties	Value	Unit
Mass Density of the Rail	7830	kg/m <sup>3</sup>
Modulus of Elasticity of the Rail	2.059 × 10 <sup>11</sup>	N/m <sup>2</sup>
Poisson's Ratio of the Rail	0.30	mm/mm
Stiffness of the Rails Pads *	5.0 × 10 <sup>7</sup>	N/m
Damping of the Rail Pads	7.5 × 10 <sup>4</sup>	N.s/m
Thickness of Concrete Slab	0.20	m
Mass Density of the Concrete Slab	2500	kg/m <sup>3</sup>
Modulus of Elasticity of the Concrete Slab **	3.6 × 10 <sup>10</sup>	N/m <sup>2</sup>
Poisson's Ratio of the Concrete Slab	0.20	mm/mm
Thickness of Self Compacting Concrete	0.09	m
Mass Density of the SC Concrete	2500	kg/m <sup>3</sup>
Modulus of Elasticity of SC Concrete **	3.4 × 10 <sup>9</sup>	N/m <sup>2</sup>
Poisson's Ratio of Self Compacting Concrete	0.2	mm/mm
Thickness of Concrete Base	0.2	m
Mass Density of the Concrete Base	2500	kg/m <sup>3</sup>
Modulus of Elasticity of the Concrete Base **	3.2 × 10 <sup>10</sup>	N/m <sup>2</sup>
Poisson's Ratio of the Concrete Base	0.2	mm/mm

\*Dynamics stiffness

\*\* Reference static value, Strain rate dependent

in LS-DYNA keyword. The enhancement factors for strain rate proposed by Comite Euro-International Du Beton (CEB) are presented in Eqs. 2 and 3 [25].

$$\eta_c = \frac{E_d}{E_s} = \left( \frac{\dot{\epsilon}}{\dot{\epsilon}_{sc}} \right)^{0.026} \tag{2}$$

$$\eta_t = \frac{E_d}{E_s} = \left( \frac{\dot{\epsilon}}{\dot{\epsilon}_{st}} \right)^{0.016} \tag{3}$$

The enhancement factors for strain rate under compression and tension are denoted as  $\eta_c$  and  $\eta_t$ , respectively.  $E_d$  and  $E_s$  stand for the dynamic and static modulus of elasticity. The effective strain rate experienced by concrete under

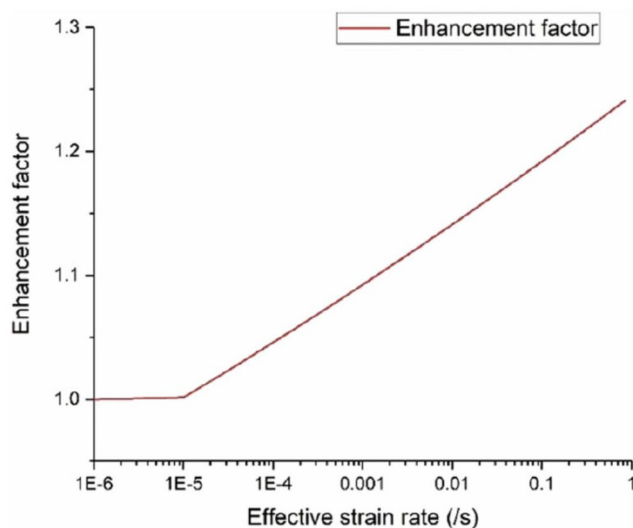


**Fig. 5** Relationship between enhancement factor and effective strain rate

dynamic loading is represented as  $\dot{\epsilon}$ , while  $\dot{\epsilon}_{st}$  and  $\dot{\epsilon}_{sc}$  represent the effective strain rates under tensile and compressive loads. Notably, the values for  $\dot{\epsilon}_{st}$  and  $\dot{\epsilon}_{sc}$  are  $3 \times 10^{-6}$  1/s and  $30 \times 10^{-6}$  1/s respectively. Winfrith concrete model proposes the use of average strain rate enhancement factors and the following Eq. 4 establishes a relationship between dynamic modulus of elasticity and strain rate [24, 26, 27].

$$\frac{E_d}{E_s} = 0.5 \times \left[ \left( \frac{\dot{\epsilon}}{3 \times 10^{-6}} \right)^{0.016} + \left( \frac{\dot{\epsilon}}{30 \times 10^{-6}} \right)^{0.026} \right] \tag{4}$$

The dynamic strain rate model is applied to incorporate the property of strain rate-dependent plasticity in concrete sleepers. The alteration in the enhancement factor due to fluctuations in effective strain rate is displayed in Fig. 5. A value of 1 is set as the lower limit for the enhancement factor. The dynamic modulus of elasticity and yield stress, expressed as functions of strain rate dependent, are utilized as inputs for the keyword “STRAIN\_RATE\_DEPENDENT\_PLASTICITY”. This keyword serves to introduce the impact of strain rate enhancement on concrete components in the model.

### Ground modelling

In this paper, the analysis of soil needs to be tailored to the different layers of soil and material properties specific to construction in Bangkok, Thailand. In particular, this research focuses on Bangkok Clay Soil, which is a common soil type in the area. Bangkok Clay Soil is complex and composed of four layers, namely Soft Clay (SC), Medium Stiff Clay (MC), Hard Stiff Clay (HC), and Sand. To accurately model this soil, 3D Finite Element Method (FEM) solid elements are used for all parts of the soil. Additionally, the soil layers

are modelled as Elastic materials. To prevent wave reflection at the edges of the ground, Perfectly Matched Layers (PML) elements are used. It effectively absorbs outgoing waves from within a computational area, ensuring these waves do not reflect back into the interior. This capability is crucial for accurate wave simulation and analysis, as it minimize the impact of boundary reflections on the results.

In the context of Bangkok’s soil composition, the characteristics tend to exhibit predominantly clay or soft soil attributes in practical scenarios. The Bangkok’s soil profile and properties used are from previous literature [28]. This classification typically encompasses depths ranging from 0 to 12 m, where the soil is generally characterized as very soft to soft clay. Subsequently, at depths spanning 12 to 27 m, the soil transitions into a state classified as medium stiff to very stiff clay. Notably, within this soil profile, a distinct layer of 1st dense sand becomes apparent. In practical construction applications, a notable technique involves leveraging this initial sand layer as the foundation for pile tips. These pile tips play a pivotal role in effectively distributing and displacing the structural forces. This study’s scope primarily addresses the uppermost layers of the ground, including the made ground Layer (Loose Soil) and the upper strata of soft clay.

The soil used for validation purposes is the original soil design from the Beijing-Shanghai High-Speed Line in China [29], which consists of five layers, namely the top clay layer, bottom clay layer, completely weathered amphibolite layer, highly weathered amphibolite layer, and weakly weathered

amphibolite layer. In field measurements, it is difficult to obtain experimental values for the different layers of the soil, making it challenging to define an accurate damping coefficient. To address this issue, Rayleigh damping of the soil was used in the simulation to approximate the damping ratio,  $C$ , as shown in Eq. 5 and to overcome the complexity of obtaining direct experimental values for ground layers [30].

$$C = \alpha M + \beta K \tag{5}$$

where  $C$ =Rayleigh damping of soil,  $M$ =Mass matrix of the structures,  $K$ =Stiffness matrix of whole model, assumed  $\alpha=0$  and  $\beta=0.0002$  to be more convenient to calculate Rayleigh Damping, or damping effect depends on the value of the stiffness of all layers of soil [21].

The comparison of material properties of soil from previous studies is illustrated in Table 6. The primary disparities lie in the dimensional aspects and characteristics of both the 1st ground and the 2nd ground. Specifically, the depth of the 1st ground has been diminished to 2.0 m, while the 2nd ground’s depth now stands at 3.0 m. This alteration stems from the notion that the influence of ground acceleration diminishes significantly with depth for soft soils such as BKK clay soil, thereby reducing our emphasis on subterranean variations.

In summary of the soil modelling adjustments, the overall soil depth has been revised from 15.0 m to 5.0 m, in accordance with the stated rationale. As detailed in Table 6,

**Table 6** Material properties of soil [29, 31]

Properties	China High-Speed Line Soil for Validation from [29]	Bangkok Clay Soil used in this study from [31]	Unit
Depth of Surface Layer of the Subgrade	0.40	0.40	m
Density of Surface Layer of the Subgrade	2300	2300	kg/m <sup>3</sup>
Elastic Modulus of Subgrade Surface Layer	5.47 × 10 <sup>5</sup>	5.47 × 10 <sup>5</sup>	N/m <sup>2</sup>
Poisson’s Ratio of Subgrade Surface Layer	0.25	0.25	mm/mm
Depth of Bottom Layer of the Subgrade	2.30	2.30	m
Density of Bottom Layer of the Subgrade	1950	1950	kg/m <sup>3</sup>
Elastic Modulus of Subgrade Bottom Layer	1.50 × 10 <sup>8</sup>	1.50 × 10 <sup>8</sup>	N/m <sup>2</sup>
Poisson’s Ratio of subgrade Bottom Layer	0.35	0.35	mm/mm
Depth of the Subgrade	2.00	2.00	m
Density of Subgrade	2100	2100	kg/m <sup>3</sup>
Elastic Modulus of the Subgrade	1.10 × 10 <sup>8</sup>	1.10 × 10 <sup>8</sup>	N/m <sup>2</sup>
Poisson’s Ratio of Subgrade	0.30	0.30	mm/mm
Depth of 1st Layer of Ground	5.0	2.0	m
Density of 1st Layer of Ground	1900.00	1835.49	kg/m <sup>3</sup>
Elastic Modulus of the 1st Layer of Ground	4.20 × 10 <sup>7</sup>	4.56 × 10 <sup>7</sup>	N/m <sup>2</sup>
Poisson’s Ratio of 1st Layer of Ground	0.30	0.20	mm/mm
Depth of 2nd Layer of Ground	10.0	3.0	m
Density of 2nd Layer of Ground	2010.00	1835.49	kg/m <sup>3</sup>
Elastic Modulus of the 2nd Layer of Ground	8.30 × 10 <sup>7</sup>	8.50 × 10 <sup>5</sup>	N/m <sup>2</sup>
Poisson’s Ratio of 2nd Layer of Ground	0.36	0.20	mm/mm

**Table 7** Properties of under sleeper pads, USPs

Properties	Value	Unit
Thickness of USPs	0.10	m
Density of USPs	1100	kg/m <sup>3</sup>
Poisson's Ratio of USPs	0.45	mm/mm
Bedding Modulus of Medium Stiff USPs	0.25	N/mm <sup>3</sup>
Bedding Modulus of Stiff USPs	0.35	N/mm <sup>3</sup>
Bedding Modulus of Very Stiff USPs	1.00	N/mm <sup>3</sup>

**Table 8** Properties of under slab mats, USMs

Properties	Value	Unit
Thickness of USMs	0.10	m
Density of USMs	700	kg/m <sup>3</sup>
Poisson's Ratio of USMs	0.35	mm/mm
Bedding Modulus of Typical USMs	0.11	N/mm <sup>3</sup>
Bedding Modulus of Medium Stiff USMs	0.15	N/mm <sup>3</sup>
Bedding Modulus of Stiff USMs	0.23	N/mm <sup>3</sup>

The most notable differences lie in the first and second layers of the ground. It is shown that significant differences are found in the deeper ground layers. China's deeper layers are much thicker and denser, with a higher elastic modulus and Poisson's ratio compared to Thailand's. These differences reflect the unique geological conditions and engineering requirements in each region [31]. Furthermore, to enhance the realism of the analysis for the transition problems under consideration, the properties of the soil from the China high-speed line have been replaced with those of soft soil, specifically Bangkok clay soil.

### Under sleeper pads (USPs) and under slab mats (USMs)

The design case of this study aims to investigate the effects of installed under sleeper pads (USPs) and under slab mats (USMs) on track transition, from the moving direction of the train at the ballasted track zone to the slab track side. Specifically, the study seeks to examine the impact of using different types of pads with varying stiffness in terms of bedding modulus on reducing track vibration and differential settlement on both the track and ground. USPs are installed underneath sleepers on ballasted track while USMs are installed on the isolation layer of slab track. To achieve these objectives, USP and USM models are utilized with solid elements, incorporating materials properties as shown in Tables 7 and 8. Different pad types are considered based on the recommended bedding modulus from previous literatures [14, 15, 32, 33].

The analysis also varies train speed in the increments of 50 km/hr, from 50 km/hr up to a maximum of 250 km/hr, to determine the critical speed and most effective mixed types of pads that can improve track stiffness while reducing track and ground vibrations. These findings will highlight

**Table 9** Validation results of train-track-soil interaction on ballasted track

Dynamic response from the analysis	Simulation results [34]	Simulation results from this study	Unit
Wheel-rail contact force	100	115	kN
Maximum displacement of rail (rail seat)	2.606	2.292	mm
Maximum displacement of rail (mid-span)	2.604	2.396	mm

**Table 10** Validation results of train-track-soil interaction on slab track

Dynamic response from the analysis	Simulation results [35]	Simulation results from this study	Unit
Wheel-rail contact force	98.7	93.36	kN
Maximum rail pad force	37.648	35.53	kN
Maximum displacement of rail	0.827	1.198	mm

the differences in mechanical properties between USMs and USPs, providing valuable insights for resilient material selection and application in various scenarios.

## Results

### Model validation

Before interpreting the results obtained in this study, the modified models are executed and validated with results from other articles. Mesh size is optimized prior to the actual simulations. The comparison of dynamic response is made in terms of the interaction between wheel-rail contact force and rail displacement to ensure the accuracy of support stiffness and track and ground modelling. In this study, the validation of both ballasted and slab tracks was performed separately using previous research results as benchmarks. For the ballasted track, the validation involved comparing simulation results for the wheel-rail contact force, maximum displacements of the rail, and concrete sleeper against previously validated Finite Element Method (FEM) results. For the slab track, the validation of the train-track interaction model focused on three key aspects: wheel-rail contact force, rail pad force, and rail displacement. Initially, the material properties were adjusted to match those used in previous studies to ensure consistency and accuracy. Once validation was achieved, the material properties were modified to reflect the specific conditions of the cases under study. Tables 9 and 10 present a comparison of simulation results from this study with previous works [34, 35], demonstrating the validation of the Train-Track-Soil interaction on both ballasted track and slab track, respectively. It is found that the results are in good agreement with previous works.



### Rail displacement

Rail displacement and track stiffness along the location of the transition zone without any pads under different train speeds, presented as in Fig. 6. The solid lines present the rail displacement while the dash lines present the track stiffness along the section. The left side of the Fig. 6 presents the responses on ballasted track while the right side shows the responses on slab track. Evidently, the stiffness of the slab track significantly surpasses that of the ballasted track, resulting in notably reduced vertical rail displacement. This substantial difference in stiffness has the potential to greatly induce differential settlement, consequently accelerating the rate of degradation. Furthermore, the correlation between increased train velocity and amplified rail displacement is observable. Therefore, a strong recommendation is made to adjust and optimize the track stiffness at this specific location.

The variations in rail displacement and track stiffness across the transition zone as in Fig. 7, with diverse resilient materials employed on either side. Similar trends are evident across all cases, except when higher train speeds are approached, resulting in amplified rail displacement and decreased track stiffness. Notably, the absence of pads leads to a distinct and abrupt shift in rail displacement and stiffness. The installation of USPs and USMs leads to the achievement of track smoothness, facilitated by the subsequent adjustment in stiffness. Although USPs may slightly elevate rail displacement, the deviations remain within acceptable limits. Furthermore, USPs offer ancillary advantages such as mitigating vibrations within the underlying

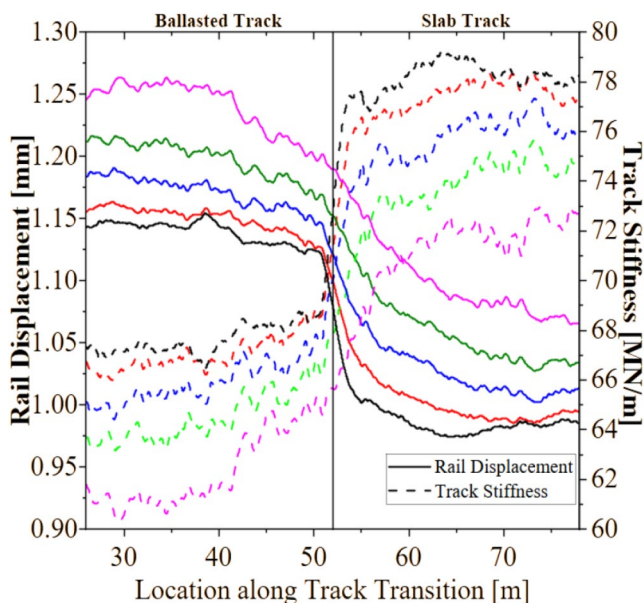


**Fig. 6** Rail displacement with track stiffness along the transition zone due to passing train with different train velocities for the controlled case (No USMs & No USPs)

strata. In contrast, for slab tracks, the installation of USMs notably enables substantial adjustments to track stiffness, rendering the track more pliable. The outcomes indicate that optimal track smoothness is achieved when utilizing typical USMs.

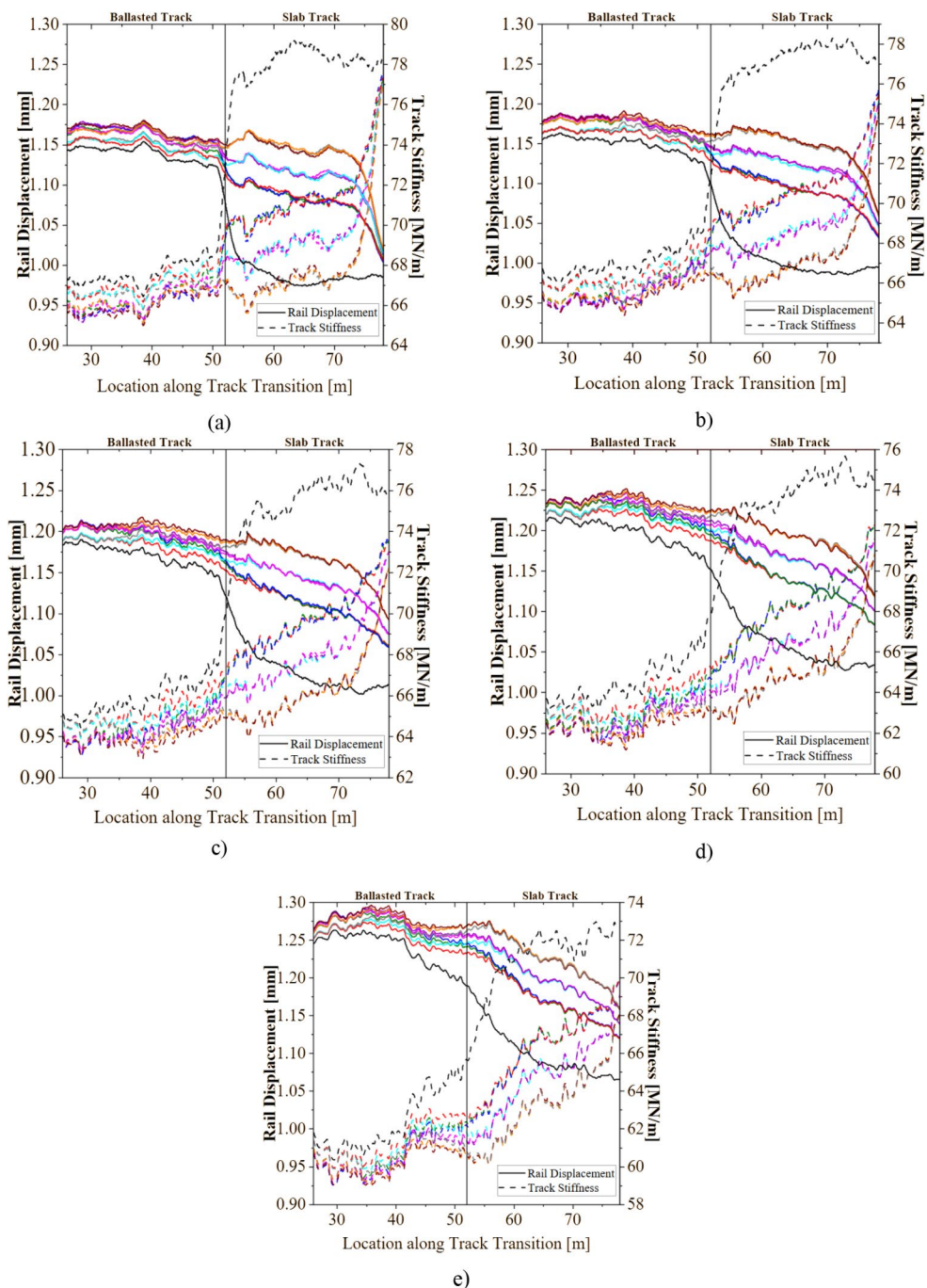
The percentage adjustment in track stiffness between two configuration zones is compared as shown in Fig. 8. This comparison involves a ballasted track with USPs installed at the 44 m position and a slab track with USMs installed at the 66 m position. The analysis considers varying stiffness values of USPs and USMs under different train speeds, with percentage values relative to the maximum difference observed in a control scenario where no USPs or USMs are installed.

The results reveal that USMs significantly adjust track stiffness in the slab track, achieving an adjustment more than 10%. In contrast, USPs in the ballasted track are less effective, leading to a slight reduction in stiffness adjustment. This indicates that USMs are more effective in optimizing track stiffness in slab tracks compared to USPs in ballasted tracks under the studied conditions.

In Fig. 9, the track stiffness gradient across different scenarios is analyzed by comparing the stiffness at the 66 m position on a slab track with the 44 m position on a ballasted track. These measurements are taken over a 20 m distance. The track stiffness gradient is calculated to evaluate the effectiveness of using mixed Under Sleeper Pads (USPs) and Under Sleeper Mats (USMs) in adjusting track stiffness at the transition zone.

To interpret the results more clearly, significant initial changes in track stiffness values were normalized. This normalization process facilitated a more precise assessment of how effectively mixed USPs and USMs achieve the desired stiffness gradient, providing insights into the impact of combined USPs and USMs on adjusting track stiffness in these critical transition areas. The baseline scenario, with no USMs or USPs, exhibits the highest stiffness gradient (1.00), indicating a sharp transition. In contrast, combinations of typical or medium stiff USMs with medium to very stiff USPs significantly reduce the gradient, achieving smoother transitions. For instance, typical USMs with very stiff USPs show the lowest gradient (0.04–0.20), demonstrating the most effective smoothing. Medium stiff USMs also effectively moderate the gradient, particularly when combined with very stiff USPs (0.22–0.34). However, configurations with stiff USMs result in higher gradients, ranging from 0.39 to 0.60, suggesting a more rigid structure that may not provide the desired smoothness in transition zones. Overall, the analysis underscores that for optimal track performance, particularly in transition zones, selecting appropriate combinations of USMs and USPs favoring typical or medium stiff USMs with stiffer USPs can effectively reduce both

**Fig. 7** Rail Displacement with track stiffness along the transition zone due to passing train: (a) 50 km/hr (b) 100 km/hr (c) 150 km/hr (d) 200 km/hr (e) 250 km/hr



track stiffness and the stiffness gradient, ensuring smoother transitions and improved track stability.

### Track responses

This section discusses the effectiveness of different types of pads in reducing stress in underlying layer, particularly on ballasted and slab tracks. The comparison is made between acceleration responses subjected to train with speed of 50–250 km/hr when using pads versus when not using pads.

Figures 10 and 11 display stress distribution for the two cases side by side, emphasizing variations at different track locations. The analysis encompasses different train speeds: 50 km/hr (lowest) and 250 km/hr (the highest). The utilization of resilient materials is evidently effective in redistributing stress and significantly diminishing concentrated stress levels on both ballasted and slab tracks.

In Fig. 12 displays the maximum stress distribution on ballasted track across the section, while Fig. 13 shows maximum stress distribution on concrete base layer in the slab

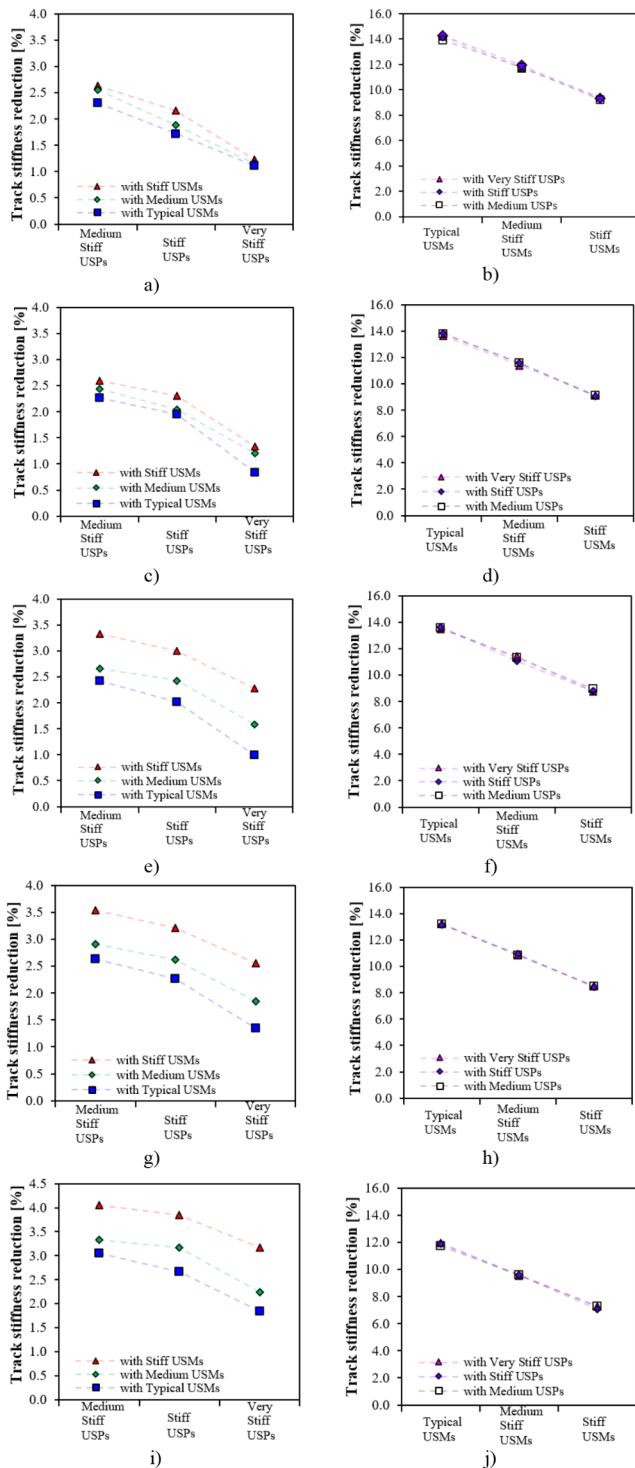


**Fig. 8** Reduction of track stiffness for mixed type of USPs and USMs (a) 50 km/hr (c) 100 km/hr (e) 150 km/hr (g) 200 km/hr (i) 250 km/hr for ballasted track and (b) 50 km/hr (d) 100 km/hr (f) 150 km/hr (h) 200 km/hr (j) 250 km/hr for slab track

track zone. Regarding the ballasted track, the results indicate that the incorporation of medium stiff USPs leads to substantially lower stress levels in comparison to the section without USPs. Although the implementation of very stiff USPs is comparatively less effective, it still demonstrates the capacity to redistribute stress and curtail maximum stress within the section. Figure 13 presents the peak stress observed across the concrete base throughout the cross-sectional area. Notably, the stress distribution can be altered, resulting in heightened stress levels at the mid span and rail seat positions, accompanied by a reduction in the overall maximum stress magnitude. This phenomenon is attributed to the alteration in the vibration pattern of the slab, consequently inducing a shift in the distribution of stress within the underlying layers.

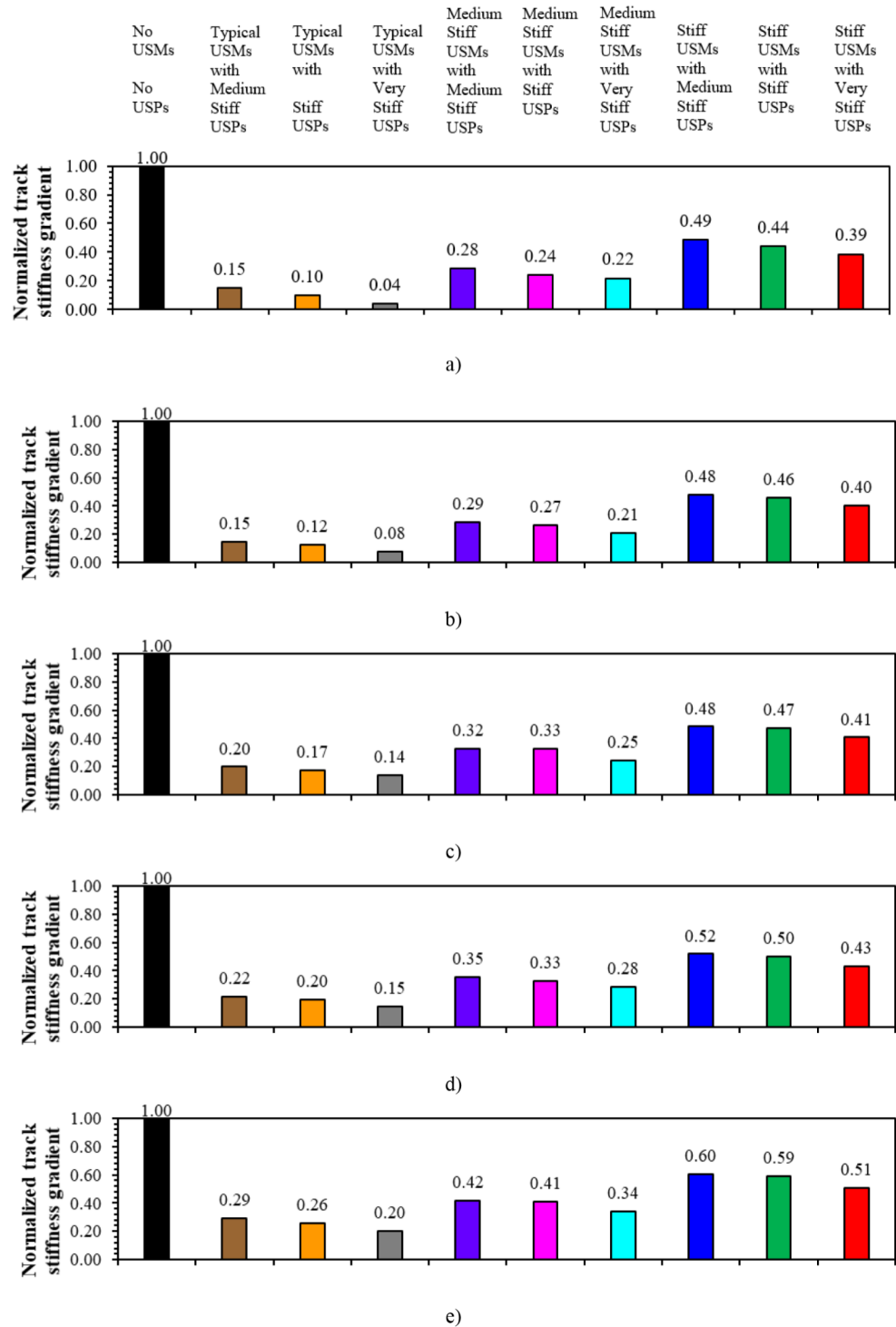
When analyzing the data for both ballasted track and slab track conditions, we constructed a graph as shown in Fig. 14 that illustrates the maximum vertical stress values at different velocities. This graph provides a visual representation of the stress distribution and highlights the varying stress levels experienced by each track type as the velocity changes. This graph provides an avenue for deeper interpretation and insights into the performance and load-bearing attributes of both ballasted and slab tracks when subjected to varying operational speeds.

To compare the reduction in stress on the layer of ballast which USPs are installed, Fig. 14a shows that there are about 3 groups based on the type of USP used. The first group, using very stiff USPs, shows a stress reduction of about 5–6%, compared to the scenario without USPs. The second group, using stiff USPs, and the third group, using medium stiff USPs, show similar results with stress reductions of approximately 12% and 14%, respectively. These results are consistent with the expected performance of different USP types. In contrast, the trends observed in concrete base are remarkably similar across all cases. A broader examination of the graph reveals that all cases demonstrate a consistent trend of increasing stress with rising train velocity. On average, the stress on the concrete base is reduced by approximately 24% across all cases compared to the scenario without USMs.

### Ground responses

As previously mentioned, while the use of resilient pads on the transition zone can reduce track acceleration and improve track stability, they may not significantly reduce ground vibrations. This section presents the ground vibration along the track transition with different types of resilient pads. Figure 15 shows the dynamic responses of ground under the train speed of 250 km/hr. It is found that ground vibration can still be observed even at considerable

**Fig. 9** Normalized track stiffness gradient for mixed type of USPs and USMs (a) 50 km/hr, (b) 100 km/hr, (c) 150 km/hr, (d) 200 km/hr, and (e) 250 km/hr



distances from the track center. The maximum acceleration is captured in both longitudinal and transverse directions.

Ground acceleration in the middle of the model for the controlled case without resilient materials and the cases with resilient materials, presented in Figs. 16 and 17 respectively. The influence of train speed on the dynamic response is prominently displayed. As the train traverses

the railway track transition at varying speeds, the ground acceleration profile exhibits distinct variations, reflecting the intricate relationship between train speed and track dynamics especially at track location. Figure 17 shows the cases with resilient materials incorporated. It is found that despite the presence of resilient materials, the overall trends in ground acceleration profiles maintain a semblance to

**Fig. 10** Vertical stress (Z-Stress) on ballast layer of ballasted track due to passing train: **(a)** No USPs, 50 km/hr train **(b)** Medium Stiff USPs, 50 km/hr train **(c)** No USPs, 250 km/hr train **(d)** Medium Stiff USPs, 50 km/hr train

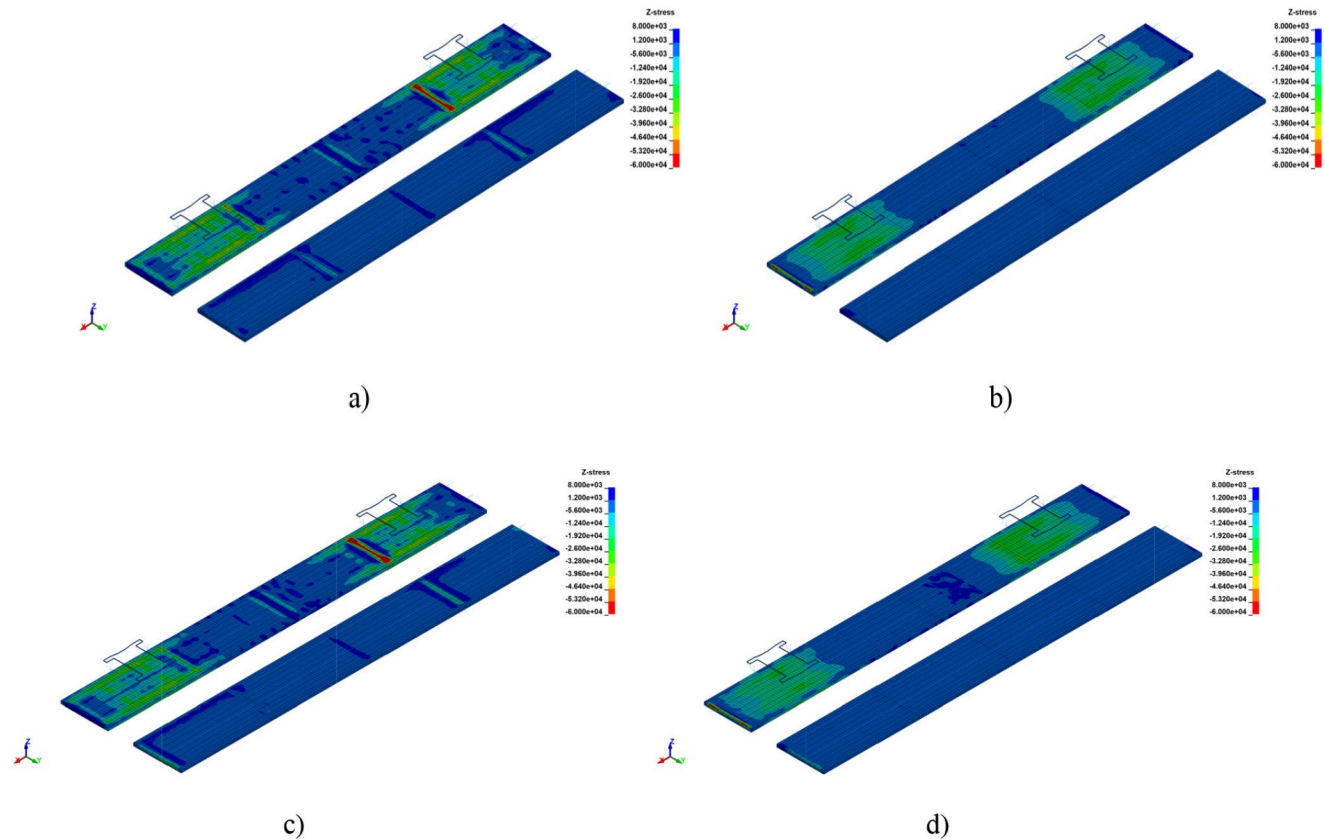
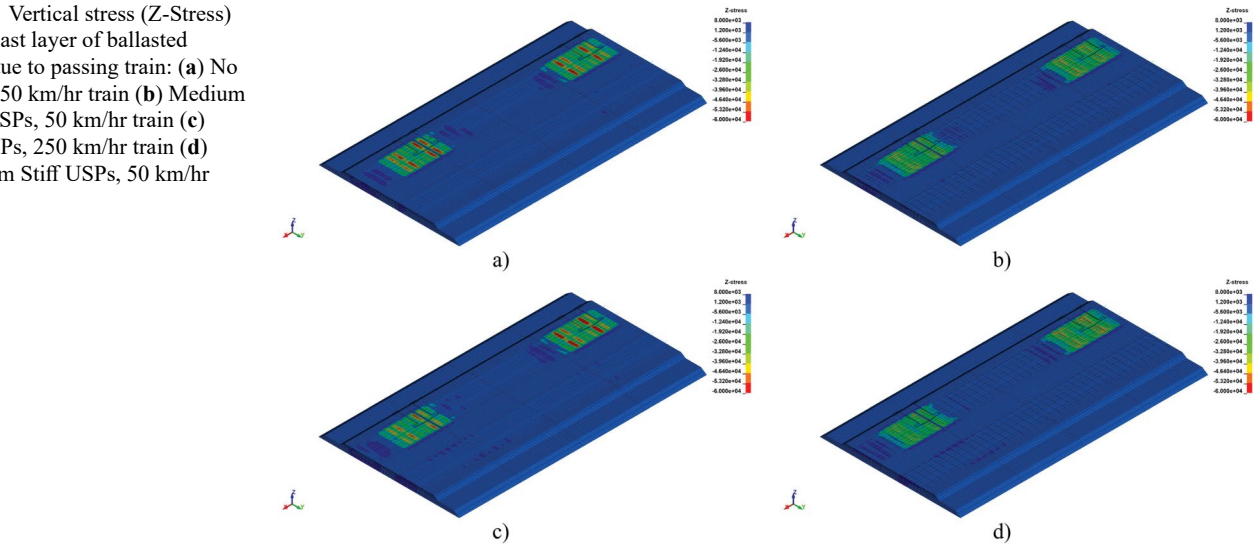
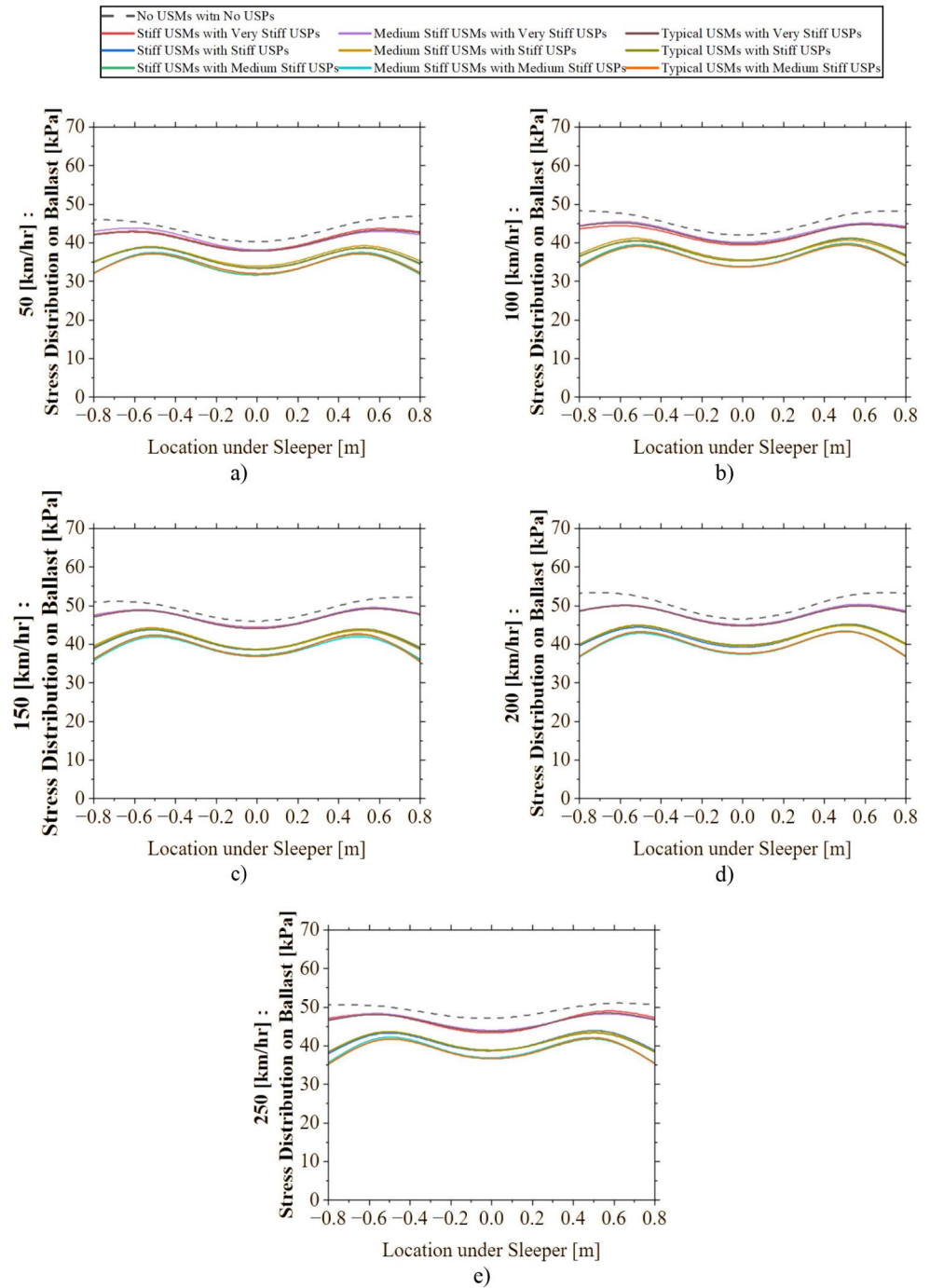


**Fig. 11** Vertical stress (Z-stress) in concrete base layer of slab track due to passing train: **(a)** No USMs, 50 km/hr train, **(b)** Medium Stiff USMs, 50 km/hr train **(c)** No USMs, 250 km/hr train **(d)** Medium Stiff USMs, 50 km/hr train

those observed in the controlled case. The consistent trends observed in Figs. 16 and 17 emphasize that while resilient materials offer advantages in specific localized aspects of dynamic response, they do not substantially deviate the global behavior from the established baseline.

In summary, as depicted in Fig. 18, varying velocities between 50 and 250 km/hr exhibit minimal disparity in maximum ground surface acceleration when utilizing different resilient materials. However, at higher velocities, a slight enhancement in ground surface vibration is discernible through the application of a mixed-type pad. Nevertheless,

**Fig. 12** Maximum stress distribution on ballast layer under passing train: **(a)** 50 km/hr **(b)** 100 km/hr **(c)** 150 km/hr **(d)** 200 km/hr and **(e)** 250 km/hr



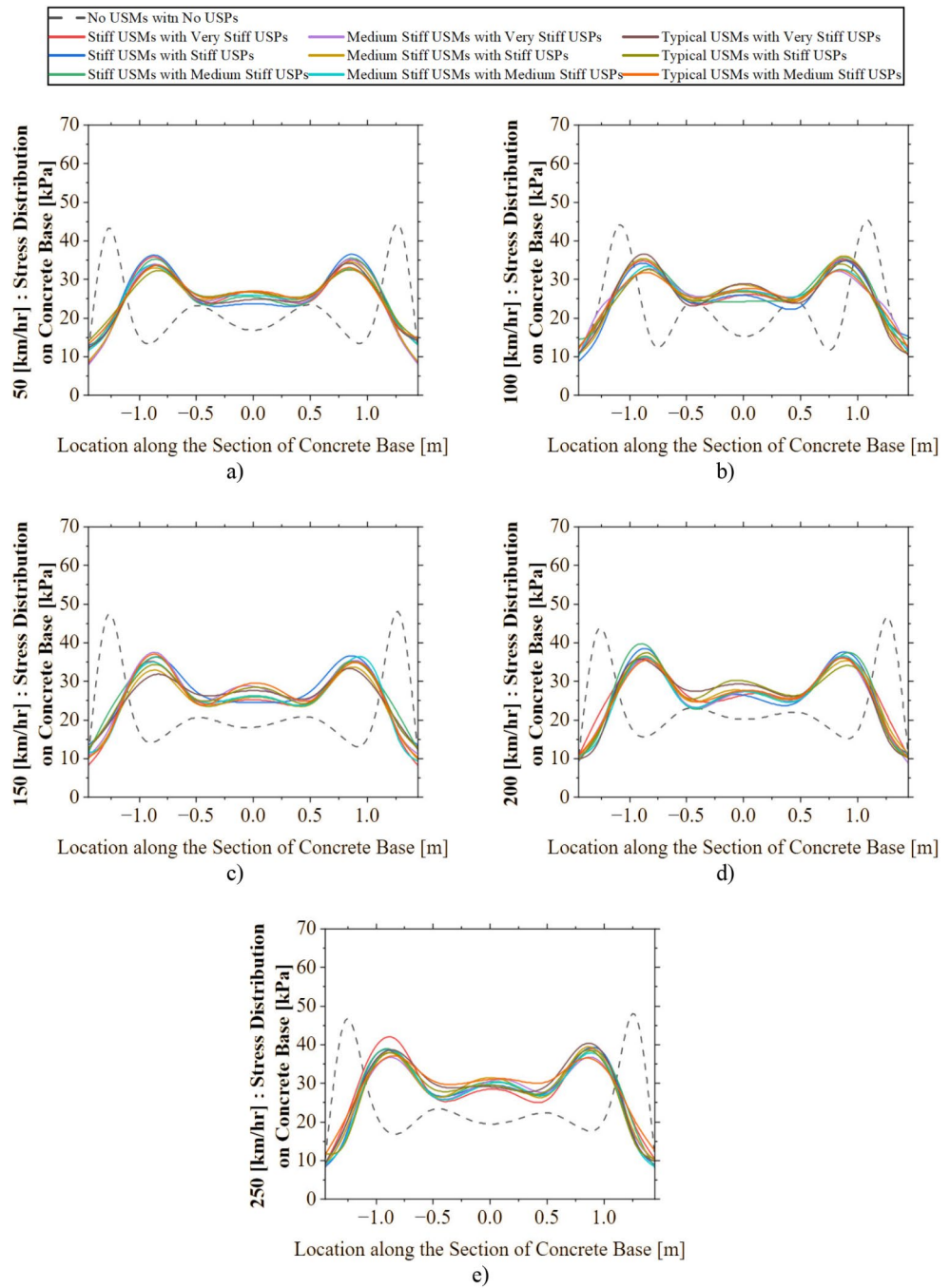
the overall discrepancy remains marginal, exerting negligible influence on the system’s vibration. In conclusion, the utilization or absence of resilient materials does not significantly impact ground surface vibration. Moreover, the operational velocity considered in this study is 250 km/h, reflecting the specific context of Thailand’s railway infrastructure. This speed does not induce resonance in the track. Previous studies have shown that the critical speed for track resonance is generally above 300 km/h [36]. To accommodate higher speeds, the track would need to be upgraded,

and the resonance phenomena, along with its shifted frequency due to the integration of resilient materials, should be thoroughly studied.

### Conclusions

The study highlights key findings related to the use of resilient materials on railway track transition zones. It is crucial to use appropriate components to improve track stiffness

**Fig. 13** Maximum stress distribution on concrete base layer under passing train: (a) 50 km/hr (b) 100 km/hr (c) 150 km/hr (d) 200 km/hr and (e) 250 km/hr



and minimize track vibrations. The use of USPs and USMs, along with carefully considered coupling methods can be effective in achieving this goal. The outcome will provide useful information for designers and engineers to improve decisions on construction and maintenance processes. Several conclusions are drawn as follows:

- The use of stiffer USPs and softer USMs (notably Very Stiff USPs and typical USMs) proves most effective in enhancing both track stiffness and rail displacement smoothness. This method facilitates the sought-after

- reduce in track stiffness for both ballasted tracks slab track. This combination can achieve a normalized track stiffness gradient between 0.04 and 0.20, significantly improving over the controlled case with a gradient of 1.00. Importantly, the impact of resilient materials on slab tracks is more pronounced in terms of adjusting track stiffness compared to ballasted tracks. This setup leads to smoother transitions and reduced abrupt stiffness changes, enhancing ride comfort and track stability.
- Medium Stiff USPs and Typical USMs (characterized by softer pads) contribute to greater stress reduction

**Fig. 14** Maximum stress on track bed layer against train velocity: (a) Ballast (b) Concrete base

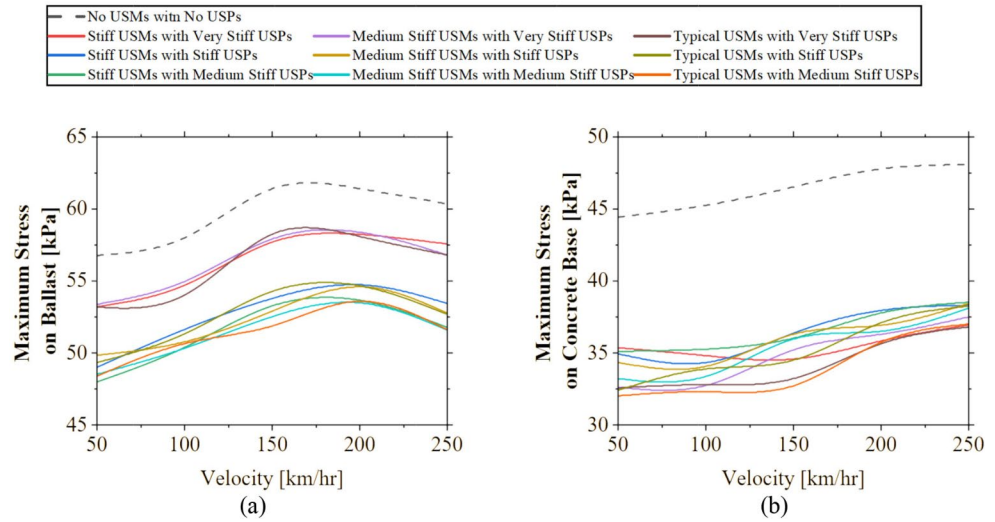


**Fig. 15** Ground dynamic response of track transition zone with typical USMs and medium stiff USPs in a 3D FEM model under train speed of 250 km/hr

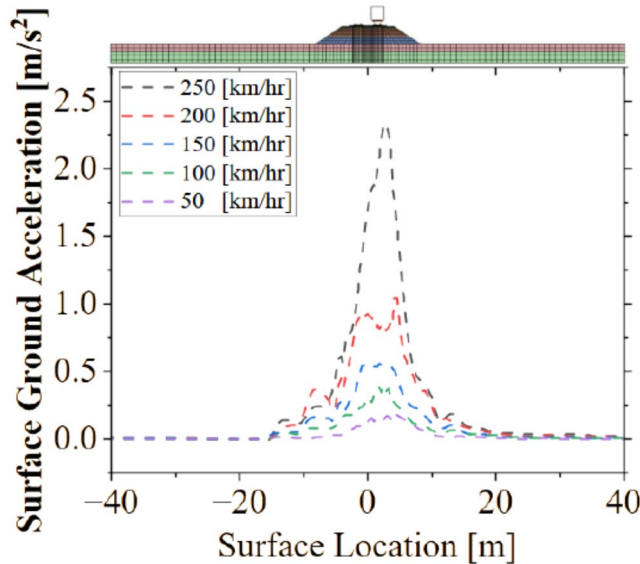
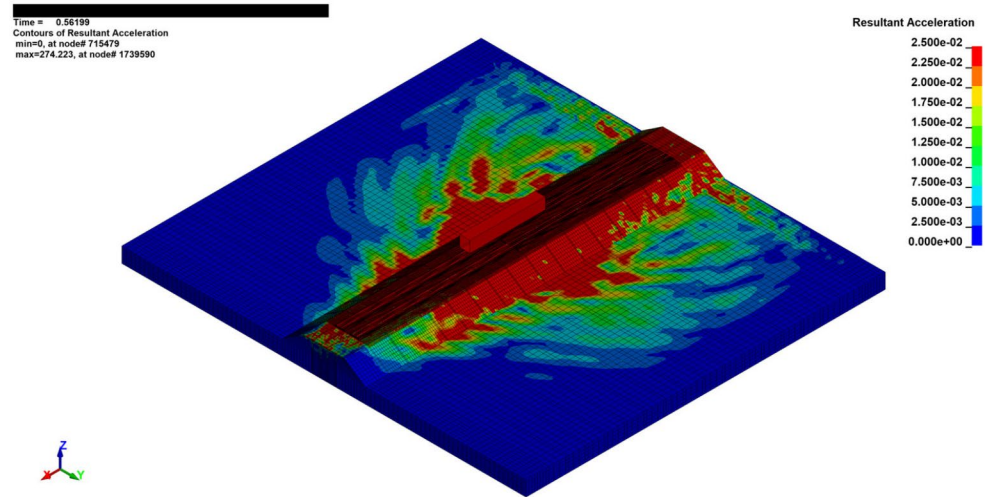


**Fig. 16** Surface ground acceleration for controlled case. (No USMs and No USPs)

within the track or substructures. However, caution must be exercised as excessively soft pads may not be conducive to effectively adjusting track stiffness, necessitating a tradeoff, as previously mentioned.

- For ballasted tracks, the utilization of USPs is recommended, though accounting for subgrade characteristics is crucial to enhance track stiffness. While USPs may not directly manipulate track stiffness or mitigate rail displacement during track transitions, they play a pivotal role in distributing forces and reducing ballast stress. Of these, medium-stiff USPs prove most efficacious in ballast stress reduction by approximately 12–14%.
- Both USPs and USMs exhibit minimal impact on reducing surface ground acceleration in the surrounding vicinity. Finally, the study underscores the significance of incorporating ground characteristics into the analysis. This is primarily attributed to the low train speed, which has not yet reached the critical speed for resonance between the train, track and the ground.



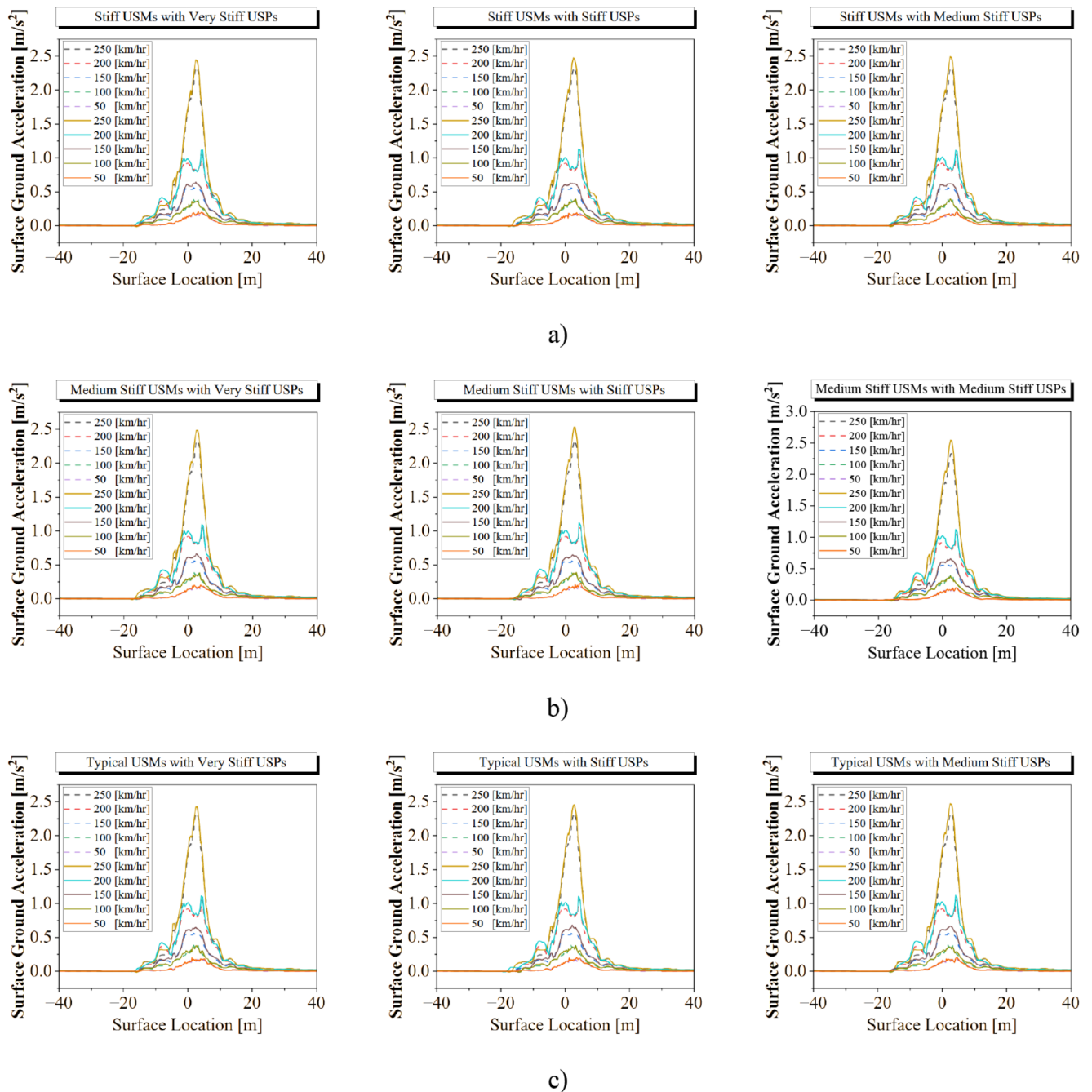


**Fig. 17** Surface ground acceleration at critical location for the case with resilient materials where controlled case (No USMs and No USPs) shown as dash line and other cases (mixed type of USMs & USPs) as solid line: (a) stiff USMs (b) medium stiff USMs (c) typical USMs

This research provides a comprehensive framework for understanding and improving the performance of railway track transition zones using resilient materials. By integrating advanced modeling techniques and dynamic analysis, it offers new perspectives on how to optimize track stiffness, manage stress distribution, and enhance overall track stability. The study’s findings are instrumental for designers and engineers in making informed decisions about the

construction and maintenance of railway infrastructure, particularly in regions with challenging soil conditions.

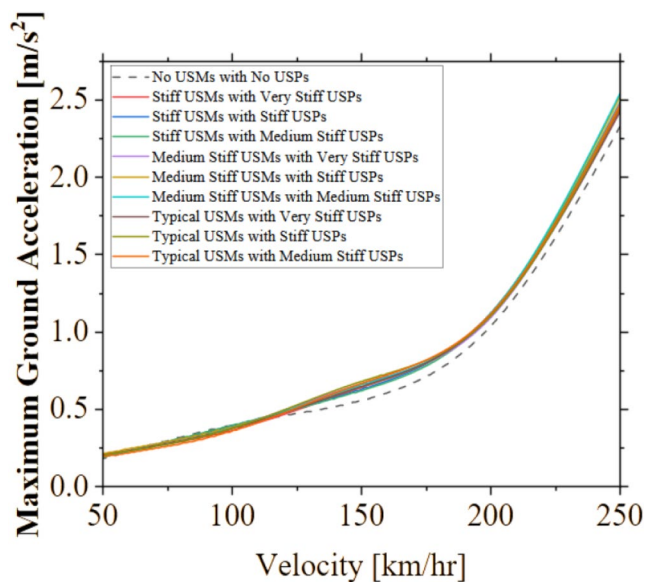


**Fig. 18** Maximum ground acceleration against train velocity

**Acknowledgements** This project is supported by Program Management Unit for Competitiveness (PMUC) Project No. C06F670025. This Research is also funded by Thailand Science research and Innovation Fund Chulalongkorn University. The second author would like to express gratitude for the postdoctoral fellowship by the Second Century Fund (C2F), Chulalongkorn University. Grants for development of new faculty staff, Ratchadaphiseksomphot Fund, Chulalongkorn University is also gratefully acknowledged. The authors wish to also thank the European Commission and UKRI Engineering and Physical Science Research Council (EPSRC) for the financial sponsorship of Re4Rail project (Grant No. EP/Y015401/1).

## Declarations

**Competing of interests** The authors declare that they have no known competing financial interests or personal relationships that could have appeared to influence the work reported in this paper.

## References

- Ngamkhanong C, Kaewunruen S, Afonso BJ, Costa (2018) State-of-the-art review of railway track resilience monitoring. *Infrastructures*, 3(1)
- Li W, Bian X (2016) Dynamic performance of pile-supported bridge-embankment transition zones under high-speed train moving loads. *Procedia Eng* 143:1059–1067
- Zuada Coelho BE (2011) Dynamics of railway transition zones in soft soils
- Kaewunruen S, Aikawa A, Remennikov AM Effectiveness of soft baseplates and fastenings to mitigate track dynamic settlement at transition zone at railway bridge approaches
- Setiawan DM (2018) Worldwide hot mix asphalt layer application and scrap rubber and bitumen emulsion studies on railway track-bed. *Semesta Teknika* 21(2):166–177
- Nassif H, Abu-Amra T, Shah N (2002) Finite element modeling of bridge approach and transition slabs
- Sañudo R et al (2016) Track transitions in railways: a review. *Constr Build Mater* 112:140–157
- Aggestam E, Nielsen JCO (2019) Multi-objective optimisation of transition zones between slab track and ballasted track using a genetic algorithm. *J Sound Vibration* 44691–112. <https://doi.org/10.1016/j.jsv.2019.01.027>
- Wang H, Markine VL (2018) Methodology for the comprehensive analysis of railway transition zones. *Computers Geotechnics* 9964–79. <https://doi.org/10.1016/j.compgeo.2018.03.001>
- Ramos A, Correia AG, Calçada R, Connolly DP (2022) Ballastless railway track transition zones: an embankment to tunnel analysis. *Transportation Geotechnics* 33100728. <https://doi.org/10.1016/j.trgeo.2022.100728>
- Shahraki M, Witt KJ (2015) 3D modeling of transition zone between ballasted and ballastless high-speed railway track. *J Traffic Transp Eng* 3(4):234–240
- Ngamkhanong C et al (2020) Dynamic train-track interactions over railway track stiffness transition zones using baseplate fastening systems. *Eng Fail Anal*, 118
- Paixão A et al (2018) Numerical simulations to improve the use of under sleeper pads at transition zones to railway bridges. *Eng Struct* 164:169–182
- Kaewunruen S et al (2018) Wet/dry influence on behaviors of closed-cell polymeric cross-linked foams under static, dynamic and impact loads. *Constr Build Mater* 187:1092–1102
- Ngamkhanong C, Kaewunruen S (2020) Effects of under sleeper pads on dynamic responses of railway prestressed concrete sleepers subjected to high intensity impact loads. *Eng Struct* 214:110604
- Zhu S, Cai C (2014) Interface damage and its effect on vibrations of slab track under temperature and vehicle dynamic loads. *Int J Non-Linear Mech* 58:222–232
- Wang M et al (2016) Experimental study on dynamic performance of typical nonballasted track systems using a full-scale test rig. *Proceedings of the Institution of Mechanical Engineers, Part F: Journal of Rail and Rapid Transit*, 231(4): pp. 470–481
- Zhi-ping Z et al (2019) Experimental study on evolution of mechanical properties of CRTS III ballastless slab track under fatigue load. *Constr Build Mater* 210:639–649
- Seraco IP (2023) Ratton Neto, contribution to Railway Track Maintenance Planning from the analysis of dynamic movements of trains. *Civil Eng J* 9(2):254–272
- Sheng X-W et al (2020) Properties of rubber under-ballast mat used as ballastless track isolation layer in high-speed railway. *Constr Build Mater* 240:117822
- Li T, Su Q, Kaewunruen S (2020) Influences of piles on the ground vibration considering the train-track-soil dynamic interactions. *Comput Geotech* 120:103455
- Qi Y, Zhou L, The Fuxing (2020) *China Standard EMU Eng* 6(3):227–233
- Liu P, Quan Y, Ding G (2019) Dynamic mechanical characteristics and Constitutive Modeling of Rail Steel over a wide range of temperatures and strain rates. *Adv Mater Sci Eng* 2019:1–15
- Li T, Su Q, Kaewunruen S (2020) Influences of dynamic material properties of slab track components on the train-track vibration interactions. *Eng Fail Anal* 115:104633
- Session C (1988) .e.-i.d.b.P., concrete structures under impact and impulsive loading: synthesis report. *Comite euro-international du beton*
- Jiang H, Chorzepa MG (2015) An effective numerical simulation methodology to predict the impact response of pre-stressed concrete members. *Eng Fail Anal* 55:63–78
- Schwer L (2011) The Winfrith concrete model: Beaty or beast. *Insights into the Winfrith concrete model*. Schwer Engineering & Consulting Services
- Likitlersuang S et al (2018) Numerical Modelling of Railway Embankments for high-speed train constructed on soft soil. *J GeoEngineering* 13:149–159

29. Wang M et al (2017) Experimental study on dynamic performance of typical nonballasted track systems using a full-scale test rig. *Proceedings of the Institution of Mechanical Engineers, Part F: Journal of Rail and Rapid Transit*, 231(4): pp. 470–481
30. Connolly DP et al (2015) Benchmarking railway vibrations—Track, vehicle, ground and building effects. *Constr Build Mater* 92:64–81
31. Chheng C, Likitlersuang S (2018) Underground excavation behaviour in Bangkok using three-dimensional finite element method. *Comput Geotech* 95:68–81
32. International Union of Railway, USP recommendations, Under Sleeper Pads, Recommendations for Use, in UIC-Leaflet, Draft Document (2013) International Union of Railway: Paris, France
33. International Union of Railway (2015) UIC Leaflet 917 guidelines for under sleeper pad. Paris, France
34. Kaewunruen S, Ngamkhanong C, Ng J (2019) Influence of time-dependent material degradation on life cycle serviceability of interspersed railway tracks due to moving train loads. *Eng Struct* 199:109625
35. Cai C-b, Zhai W-m, Wang K-y (2006) Calculation and assessment analysis of the dynamic performance for slab track on Sui-Yu railway. *China Railway Sci* 27(4):17–21
36. Raj A et al (2023) Nonlinear dynamic responses of ballasted railway tracks using concrete sleepers incorporated with reinforced fibres and pre-treated crumb rubber. *Nonlinear Eng*, 12(1)

**Publisher's Note** Springer Nature remains neutral with regard to jurisdictional claims in published maps and institutional affiliations.

Springer Nature or its licensor (e.g. a society or other partner) holds exclusive rights to this article under a publishing agreement with the author(s) or other rightsholder(s); author self-archiving of the accepted manuscript version of this article is solely governed by the terms of such publishing agreement and applicable law.